

# Strongly Hydrogen-Bonded Water Molecule Present near the Retinal Chromophore of *Leptosphaeria* Rhodopsin, the Bacteriorhodopsin-like Proton Pump from a Eukaryote<sup>†</sup>

Masayo Sumii,<sup>‡</sup> Yuji Furutani,<sup>‡,§</sup> Stephen A. Waschuk,<sup>||</sup> Leonid S. Brown,<sup>||</sup> and Hideki Kandori<sup>\*,‡,§</sup>

Department of Materials Science and Engineering, Nagoya Institute of Technology, Showa-ku, Nagoya 466-8555, Japan, Core Research for Evolutional Science and Technology (CREST), Japan Science and Technology Corporation, Kyoto 606-8502, Japan, and Department of Physics, University of Guelph, Guelph, Ontario N1G 2W1, Canada

Received July 13, 2005; Revised Manuscript Received September 3, 2005

**ABSTRACT:** *Leptosphaeria* rhodopsin (LR) is an archaeal-type rhodopsin found in fungi, and is the first light-driven proton-pumping retinal protein from eukaryotes. LR pumps protons in a manner similar to that of bacteriorhodopsin (BR), a light-driven proton pump of haloarchaea. The amino acid sequence of LR is more homologous to that of *Neurospora* rhodopsin (NR) than BR, whereas NR has no proton-pumping activity. These facts raise the question of how the proton-pumping function is achieved. In this paper, we studied structural changes of LR following the retinal photoisomerization by means of low-temperature Fourier transform infrared (FTIR) spectroscopy, and compared the obtained spectra with those for BR and NR. While the light-induced photoisomerization from the all-*trans* to 13-*cis* form was commonly observed among LR, BR, and NR, we found that the structural changes of LR are closer to those of BR than to those of NR in terms of detailed vibrational bands of retinal and protein. The most prominent difference was seen for the water O–D stretching vibrations (measured in D<sub>2</sub>O). LR exhibits an O–D stretch of water at 2257 cm<sup>−1</sup>, indicating the presence of a strongly hydrogen-bonded water molecule. Such strongly hydrogen-bonded water molecules (O–D stretch at <2400 cm<sup>−1</sup>) were observed for BR, but not for NR. Comprehensive studies of BR mutants and archaeal rhodopsins have revealed that strongly hydrogen-bonded water molecules are found only in the proteins exhibiting proton-pumping activity, suggesting that strongly hydrogen-bonded water molecules and transient weakening of their binding are essential for the proton-pumping function of rhodopsins. This observation for LR provided additional experimental evidence of the correlation between strongly hydrogen-bonded water molecules and proton-pumping activity of archaeal rhodopsins.

*Leptosphaeria* rhodopsin (LR)<sup>1</sup> is a membrane retinal-binding protein which belongs to the type I rhodopsin family (1, 2). Type I rhodopsins contain all-*trans*-retinal bound to a lysine side chain roughly in the middle of the seventh transmembrane helix via a protonated Schiff base, but are not otherwise homologous to visual pigments (type II rhodopsins). The retinal chromophore experiences all-*trans* to 13-*cis* photoisomerization followed by a chain of thermal relaxations called the photocycle. The protein moiety of type I rhodopsins responds to the changes in the retinal geometry with its own conformational changes which serve the purpose

of ion transport or signaling (reviewed in ref 3). The first major function of type I rhodopsins is ion transport as exemplified by light-driven pumping of protons or chloride. The second major function is photosensory transduction, where optical signals are transformed into conformational changes and communicated to a transducer protein mediating phototaxis or other responses to light. There is also a special case of rhodopsins from *Chlamydomonas*, where the type I rhodopsin domain is part of a much larger protein in which it regulates passive transport of protons or calcium (4, 5).

Type I rhodopsins were first discovered in halobacteria, so this protein family is sometimes called the family of rhodopsins of the haloarchaeal type (1). Halobacterial rhodopsins are very well studied, and the halobacterial genome contains genes encoding four related proteins (6): bacteriorhodopsin (BR), halorhodopsin (HR), sensory rhodopsin (SR, also called sensory rhodopsin I, SR-I), and phoborhodopsin (pR, also called sensory rhodopsin II, SR-II). BR and HR are light-driven ion pumps, which act as an outward proton pump and an inward Cl<sup>−</sup> pump, respectively (7–9). On the other hand, SR and pR are photoreceptors of halobacteria mediating attractant and repellent responses in phototaxis, respectively (10–12). Even though physiological and biochemical data suggested that type I rhodopsins may

<sup>†</sup> This work was supported in part by grants from Japanese Ministry of Education, Culture, Sports, Science, and Technology to H.K., by Research Fellowships from the Japan Society for the Promotion of Science for Young Scientists to Y.F., and by the NSERC, PREA, and Research Corporation grants to L.S.B.

\* To whom correspondence should be addressed. Phone and fax: 81-52-735-5207. E-mail: kandori@nitech.ac.jp.

<sup>‡</sup> Nagoya Institute of Technology.

<sup>§</sup> Japan Science and Technology Corp.

<sup>||</sup> University of Guelph.

<sup>1</sup> Abbreviations: LR, *Leptosphaeria* rhodopsin; BR, bacteriorhodopsin; NR, *Neurospora* rhodopsin; ppR, *pharaonis* phoborhodopsin; LR<sub>K</sub>, K intermediate of LR; BR<sub>K</sub>, K intermediate of BR; NR<sub>K</sub>, K intermediate of NR; HOOP, hydrogen out-of-plane; DMPC, 1,2-dimyristoyl-*sn*-glycero-3-phosphocholine; DMPA, 1,2-dimyristoyl-*sn*-glycero-3-phosphate.

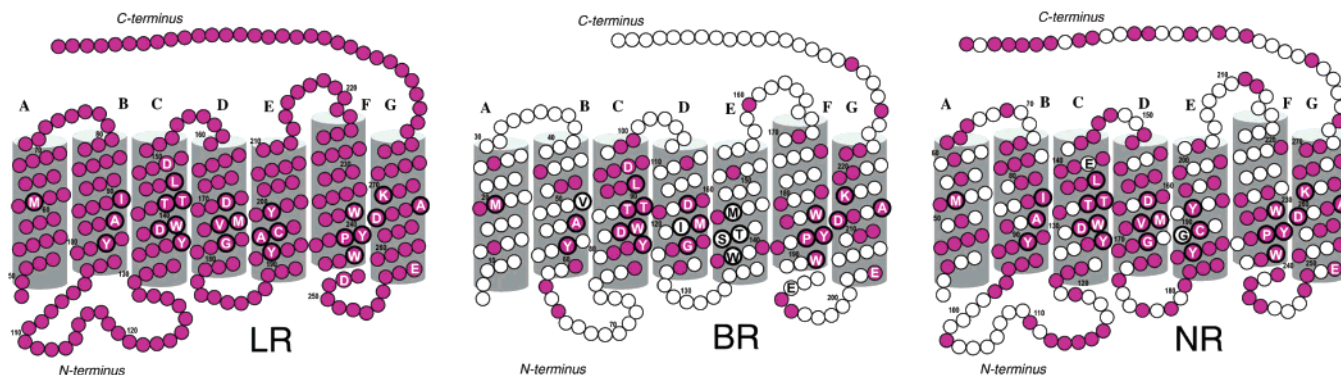


FIGURE 1: Comparison of amino acid sequences of bacteriorhodopsin (BR) and the expressed portions of *Leptosphaeria* rhodopsin (LR) and *Neurospora* rhodopsin (NR). The transmembrane topology is based on the crystallographic three-dimensional model of BR (63). The sequence alignment was done using CLUSTALW (64). The residues identical to those of LR are colored purple. The 25 bold circles compose the retinal binding site within 5 Å of the chromophore in the BR structure (63), where single letters in a circle denote the residues. In addition, three important residues in the proton pathway of BR (Asp96, Glu194, and Glu204) are shown by single letters for both LR (Asp150, Asp248, and Glu258) and NR (Glu142, deleted, and Glu251).

exist in organisms other than halobacteria, only very recently have several genome sequencing projects convincingly demonstrated the presence of rhodopsins of the haloarchaeal type not only in Archaea but also in Bacteria and Eukaryota (reviewed in refs 1, 3, and 13). Eubacterial rhodopsins were found in both  $\gamma$ - and  $\alpha$ -proteobacteria (14, 15) as well as in cyanobacteria (16). In eukaryotes, type I rhodopsins were found in fungi (17), green algae (4, 5), dinoflagellates (18), and cryptomonads (3).

Both LR and another fungal type I rhodopsin from *Neurospora* (NR) were recently investigated (2, 19–21). Figure 1 shows that the levels of identity of amino acids between LR and BR and between LR and NR are 25.7 and 55.8%, respectively. It is reasonable that LR is more homologous to NR than BR from the evolutionary point of view. On the other hand, amino acid residues along the proton pathway in BR are highly conserved for both LR and NR. They include Thr46, Ala53, Tyr57, Arg82, Asp85, Trp86, Thr89, Leu93, Trp182, Tyr185, Glu204, and Asp212 (using numbering for BR) (Figure 1). Some exceptions are as follows. Val49 in BR is replaced with Ile in LR and NR. Asp96 is replaced with Glu in NR. Glu194 is replaced with Asp in LR, while it is deleted in NR (Figure 1). These facts suggested that both LR and NR may function as light-driven proton pumps similar to BR. It was however found that NR does not pump protons (20), suggesting that the reprotonation switch is not functional in NR. In contrast, it was revealed that LR pumps protons in a manner similar to that of BR (22). Thus, LR and NR (in comparison to each other and BR) are a good system for revealing the structural elements necessary for proton pumping by rhodopsins.

Previously, we have studied protein structure and structural changes of several archaeal rhodopsins by means of low-temperature Fourier transform infrared (FTIR) spectroscopy. Newly developed measurements in a frequency region detecting X–H and X–D (X = O or N) stretching vibrations (4000–1800  $\text{cm}^{-1}$ ) provided new information about the hydrogen bonding network, including internal water molecules (23). In fact, comparing the K intermediate (BR<sub>K</sub>) minus BR difference spectra recorded with D<sub>2</sub>O or D<sub>2</sub><sup>18</sup>O in the X–D stretching region (2700–1800  $\text{cm}^{-1}$ ) enabled us to assign the O–D stretching vibrations of water molecules not only with weak hydrogen bonding (at >2500  $\text{cm}^{-1}$ ) but

also with strong hydrogen bonding (at <2400  $\text{cm}^{-1}$ ) (24). Mutational study showed that one of the O–D stretches (2171  $\text{cm}^{-1}$ ) originates from a bridge water molecule between the Schiff base and its counterion (Asp85) (25). Hydration switch of the water plays an important role in the proton transfer reactions in BR (26). Interestingly, comprehensive studies of BR mutants and other rhodopsins have revealed that strongly hydrogen-bonded water molecules are found only in the proteins exhibiting proton-pumping activity (24, 27–30). This suggests that a strongly hydrogen-bonded water molecule that bridges the Schiff base and its counterion is essential for the proton-pumping function. While NR does not have such strongly hydrogen-bonded water molecules and does not pump protons (31), what is the case for LR, which is a proton pump?

In this work, we studied low-temperature FTIR characteristics of the K intermediate of LR by comparing them with those of BR, and paying special attention to the bands of bound water, retinal Schiff base, and retinal polyene chain. This study expands FTIR characterization of LR to earlier intermediates, complementing the previous report on the late intermediates (22). It reveals important structural differences among BR, LR, and NR. In particular, a strongly hydrogen-bonded water molecule was observed for LR, which was similarly observed for BR, but not for NR. This observation for LR is entirely consistent with our finding of the correlation between strongly hydrogen-bonded water molecules and proton-pumping activity of archaeal rhodopsins.

## MATERIALS AND METHODS

**Expression of *Leptosphaeria* Rhodopsin in *Pichia pastoris*.** The *Leptosphaeria maculans ops* gene was modified and cloned into the pHIL-S1 vector in a manner similar to the procedure previously used for *Neurospora* rhodopsin (NR) (19). Briefly, *L. maculans ops* was modified such that *Leptosphaeria ops* was N-terminally truncated (48 residues) with a 6 × His tag added to the C-terminus (22). The protein was expressed in the methylotrophic yeast *P. pastoris*, strain GS115, following our optimized procedure for NR (31). During expression in *P. pastoris*, 5  $\mu\text{M}$  all-*trans*-retinal (Sigma) was added to the growth medium at approximately 24 h following induction with methanol.

**Purification and Reconstitution into Liposomes.** Breakage of *P. pastoris* cells, solubilization of the membranes, and purification and concentration of LR followed our methods previously used for NR (31). For reconstitution into liposomes, solubilized Ni-NTA-purified LR was added to preformed DMPC/DMPA (9:1) liposomes at a 3:1 lipid:protein ratio (w/w). Reconstitution by detergent (Triton X-100) removal was done using Bio-Beads SM-2 (Bio-Rad), as described elsewhere (31). Liposomes were washed repeatedly by centrifugation with 50 mM Na<sub>2</sub>SO<sub>4</sub> and 50 mM K<sub>2</sub>SO<sub>4</sub> at speeds of 40000g and frozen for further use.

**HPLC Analysis.** Extraction of retinal oxime from the sample in DM solution was carried out with hexane after denaturation by methanol and 500 mM hydroxylamine as described previously (32). A high-performance liquid chromatograph was equipped with a silica column (6 mm × 150 mm, YMC-A012-3). The solvent was composed of 12% (v/v) ethyl acetate and 0.12% (v/v) ethanol in hexane, and the flow rate was 1.0 mL/min. The molar compositions of the retinal isomers were calculated from the areas of the peaks in the HPLC patterns.

**FTIR Spectroscopy.** FTIR spectroscopy was performed as described previously (28, 33). The LR sample reconstituted into DMPC/DMPA liposomes was washed three times with 2 mM phosphate buffer (pH 7). The pellet was resuspended in the same buffer, and the concentration was adjusted to ~2 OD units at 535 nm per milliliter. An 80  $\mu$ L aliquot was deposited on a BaF<sub>2</sub> window with a diameter of 18 mm and dried in a glass vessel that was evacuated with an aspirator.

The dark-adapted LR contains predominantly all-*trans*-retinal with a small portion of 13-*cis*-retinal. The LR sample was hydrated with H<sub>2</sub>O, D<sub>2</sub>O, or D<sub>2</sub><sup>18</sup>O. The sample was then placed in a cell in an Oxford DN-1704 cryostat mounted in the Bio-Rad FTS-40 spectrometer. The cryostat was equipped with an Oxford ITC-4 temperature controller, and the temperature was regulated with 0.1 K precision.

Illumination with 500 nm light at 77 K for 2 min converted LR to LR<sub>K</sub>. Since LR<sub>K</sub> was completely reconverted to LR upon illumination with >600 nm light for 1 min, as evidenced by the spectral shape and amplitude which is a mirror image of that for the LR to LR<sub>K</sub> transition, cycles of alternating illumination with 500 and >600 nm light were repeated a number of times. The difference spectrum was calculated from two spectra constructed from 128 interferograms taken before and after the illumination; 56 difference spectra obtained in this way were averaged to produce the LR<sub>K</sub> minus LR spectrum. As linear dichroism experiments revealed the random orientation of LR molecules in the liposome film, an IR polarizer was not used.

BR<sub>K</sub> minus BR difference spectra were taken from Kandori et al. (23) and Tanimoto et al. (26), and NR<sub>K</sub> minus NR spectra were taken from Furutani et al. (31). Since BR molecules are highly oriented in the film, unlike LR, the data with a window tilting angle of 53.5° in polarized FTIR spectroscopy were used for comparison.

## RESULTS

It is well-known that there is a correlation between isomeric state in the dark and function for archaeal rhodopsins. Light-driven ion pumps, such as BR and HR, contain both 13-*cis*- and all-*trans*-retinal in the dark state, but become

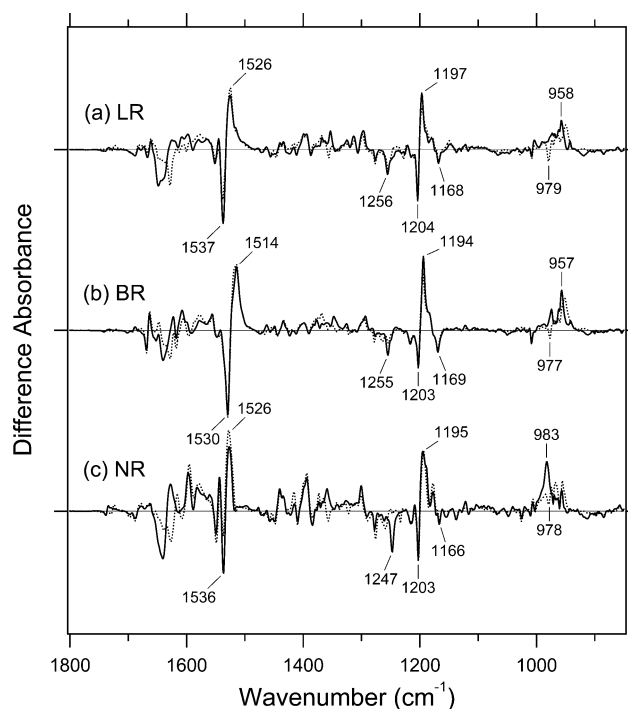


FIGURE 2: LR<sub>K</sub> minus LR (a), BR<sub>K</sub> minus BR (b), and NR<sub>K</sub> minus NR (c) spectra in the 1800–850 cm<sup>-1</sup> region measured at pH 7 and 77 K. The sample was hydrated with H<sub>2</sub>O (—) or D<sub>2</sub>O (···). Spectra in panels b and c are reproduced from Furutani et al. (31). One division of the y-axis corresponds to 0.009 absorbance unit.

predominantly all-*trans* when light-adapted (34, 35). In contrast, phototaxis proteins such as pR and sR contain only all-*trans*-retinal in the dark (36, 37). This HPLC analysis showed that LR contains mostly all-*trans*-retinal in the dark (97%) (data not shown). This observation by HPLC is consistent with the previous Raman study, which concluded that the dark-adapted LR contains predominantly all-*trans*-retinal (22). In contrast, by HPLC analysis, we confirmed that the chromophore configuration of NR is 48% all-*trans* and 52% 13-*cis* in the dark (data not shown). These results suggest that the isomeric composition of the dark-adapted states varies among type I rhodopsins and does not necessarily correlate with their functions.

**Measurement of the LR<sub>K</sub> minus LR Difference Spectra.** Figure 2a shows the LR<sub>K</sub> minus LR difference spectra measured at 77 K. The ethylenic stretching vibration at 1537 (–)/1526 (+) cm<sup>-1</sup> implies that LR is converted to a red-shifted intermediate (38), LR<sub>K</sub>, upon light absorption at 77 K. There are negative bands at 1256, 1204, and 1168 cm<sup>-1</sup> in the C–C stretching region and at 1010 cm<sup>-1</sup> in the HOOP region, which were also detected in the reported Raman spectra (22). These spectral features are similar to those of BR (Figure 2b) and NR (Figure 2c), suggesting that the LR to LR<sub>K</sub> conversion is accompanied by the retinal photoisomerization from the all-*trans* to the 13-*cis* form. However, it is clear that the spectrum of LR is closer in its shape to that of BR than that of NR, which we compare in detail below.

**Comparison of the Vibrational Bands of the Retinal Chromophore among LR, BR, and NR.** Figure 3 compares the LR<sub>K</sub> minus LR (a), BR<sub>K</sub> minus BR (b), and NR<sub>K</sub> minus NR (c) spectra in the 1290–1130 cm<sup>-1</sup> region. This frequency region includes the C–C stretching and the vinyl CCH rocking vibrations of the retinal chromophore. Negative



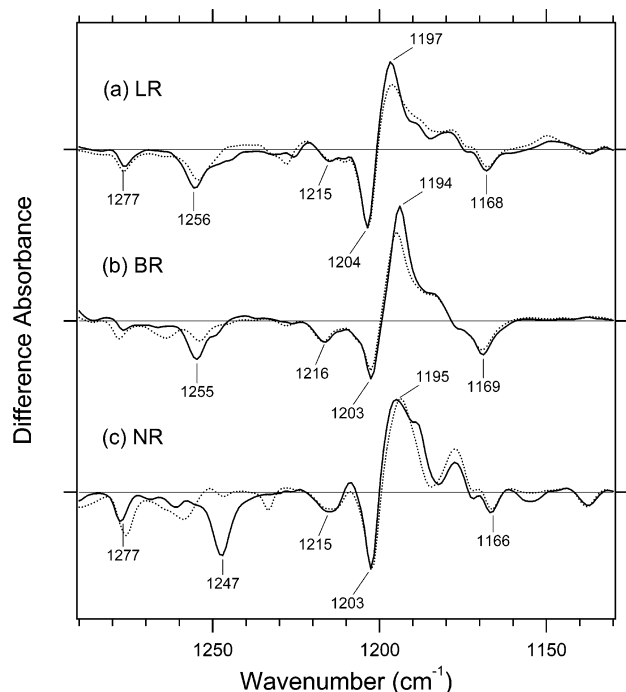


FIGURE 3:  $LR_K$  minus LR (a),  $BR_K$  minus BR (b), and  $NR_K$  minus NR (c) spectra in the 1290–1130  $\text{cm}^{-1}$  region, being reproduced and expanded from Figure 2. This frequency region corresponds to C–C stretching vibrations and C–H, N–H in-plane rocking vibrations of the retinal chromophore. The sample was hydrated with  $\text{H}_2\text{O}$  (—) or  $\text{D}_2\text{O}$  (···). One division of the y-axis corresponds to 0.0055 absorbance unit.

bands in BR at 1255, 1216, 1203, and 1169  $\text{cm}^{-1}$  can be attributed to the C–C stretching vibrations of the retinal chromophore at the C12–C13, C8–C9, C14–C15, and C10–C11 single bonds, respectively (Figure 3b) (39, 40). The negative 1255  $\text{cm}^{-1}$  band is composed of a mixture of  $\text{D}_2\text{O}$ -insensitive C12–C13 stretching and  $\text{D}_2\text{O}$ -sensitive lysine rocking vibrations (41, 42). The positive 1194  $\text{cm}^{-1}$  band of BR originates from C14–C15 and C10–C11 stretches (43). Analogous spectral features were observed for LR (Figure 3a) and NR (Figure 3c), indicating a similar chromophore conformation. In the case of LR, we tentatively assigned the bands at 1256 (—), 1215 (—), 1204 (—), and 1168 (—)  $\text{cm}^{-1}$  as a mixture of the C12–C13 stretch and lysine rock, and the C8–C9, C14–C15, and C10–C11 stretches, respectively. It should be noted that the C–C stretching vibrations of LR are closer to those of BR than those of NR. The frequencies are almost identical between LR and BR, whereas the C10–C11 (1166  $\text{cm}^{-1}$ ) and C12–C13 and lysine rock (1247  $\text{cm}^{-1}$ ) stretches of NR are different in frequency from those of LR and BR (20, 31). This result suggests that the chromophore structure of NR is different from those of LR and BR in the middle of the retinal.

Figure 4 shows the  $LR_K$  minus LR (a),  $BR_K$  minus BR (b), and  $NR_K$  minus NR (c) spectra in the 1035–900  $\text{cm}^{-1}$  region. It is well-known that the hydrogen out-of-plane (HOOP) vibrations of the retinal chromophore appear in this region, and HOOP modes provide information about chromophore distortions (39, 44–47). The  $\text{D}_2\text{O}$ – $\text{H}_2\text{O}$  exchange-insensitive negative peak at 1009  $\text{cm}^{-1}$  in Figure 4b was assigned as the symmetric in-plane methyl rocking combination involving mainly the methyl groups at C9 and C13 positions in BR (42). The 977  $\text{cm}^{-1}$  band is observed for

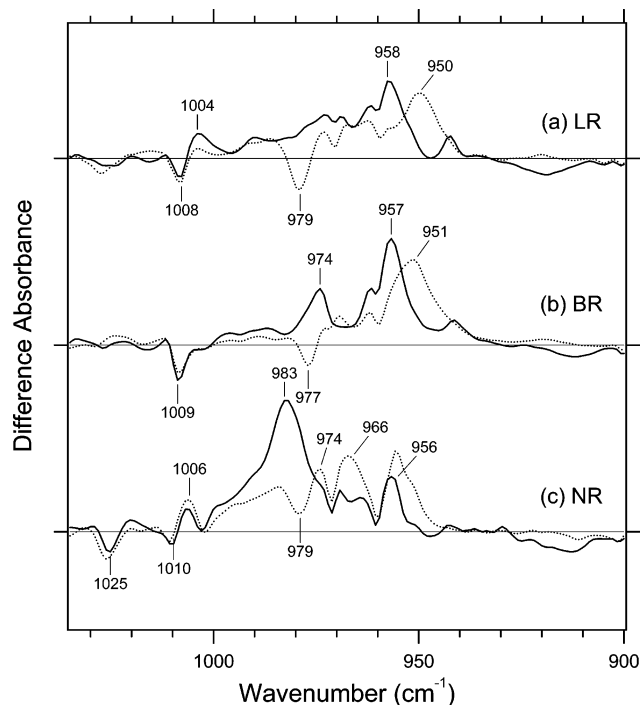


FIGURE 4:  $LR_K$  minus LR (a),  $BR_K$  minus BR (b), and  $NR_K$  minus NR (c) spectra in the 1035–900  $\text{cm}^{-1}$  region, being reproduced and expanded from Figure 2. This frequency region corresponds to hydrogen out-of-plane (HOOP) vibrations of the retinal chromophore. The sample was hydrated with  $\text{H}_2\text{O}$  (—) or  $\text{D}_2\text{O}$  (···). One division of the y-axis corresponds to 0.0035 absorbance unit.

the  $\text{D}_2\text{O}$ -treated samples only, and is assigned as the N–D in-plane rocking vibration downshifted from 1348  $\text{cm}^{-1}$  upon hydration with  $\text{D}_2\text{O}$ , consistent with the recent Raman observation of the same band at 979  $\text{cm}^{-1}$  (22). The appearance of a sharp peak at 957  $\text{cm}^{-1}$  is characteristic of the  $BR_K$  minus BR spectrum, and the  $\text{D}_2\text{O}$ -sensitive bands at 974 and 957  $\text{cm}^{-1}$  were assigned as HOOP vibrations of the C15–H and N–H bonds (40). This result indicates that the retinal distortions upon  $BR_K$  formation are localized in the Schiff base region. More complex spectral features were observed in the  $NR_K$  minus NR spectra (Figure 4c), which look similar to those of *ppR* (33). While the  $\text{D}_2\text{O}$ -sensitive intense band at 983  $\text{cm}^{-1}$  can be attributed to the HOOP vibrations of the C15–H and/or N–H bonds, we also observed the  $\text{D}_2\text{O}$ -insensitive bands at 974, 966, and 956  $\text{cm}^{-1}$ . The appearance of the  $\text{D}_2\text{O}$ -insensitive HOOP modes in NR is more similar to that of *ppR* than to that of BR, suggesting that specific distortions occur in the middle of the chromophore (31).

Figure 4a clearly shows that the spectral features observed for LR are closer to those of BR rather than those of NR. The  $\text{D}_2\text{O}$ -insensitive negative peak at 1008  $\text{cm}^{-1}$  can be assigned to the symmetric in-plane methyl rocking combination involving mainly the methyl groups at C9 and C13 in LR (40). The corresponding positive band may be located at 1004  $\text{cm}^{-1}$ , though half of the intensity of this band is reduced in  $\text{D}_2\text{O}$ . The negative 979  $\text{cm}^{-1}$  band probably corresponds to the negative band at 977  $\text{cm}^{-1}$  in BR (Figure 4b), being able to be assigned to the N–D in-plane rocking vibration downshifted from 1344  $\text{cm}^{-1}$  upon hydration with  $\text{D}_2\text{O}$ . The appearance of a sharp peak at 958  $\text{cm}^{-1}$  and its downshift to 950  $\text{cm}^{-1}$  in  $\text{D}_2\text{O}$  (Figure 4a) are very similar to the case of BR (Figure 4b). These results strongly suggest

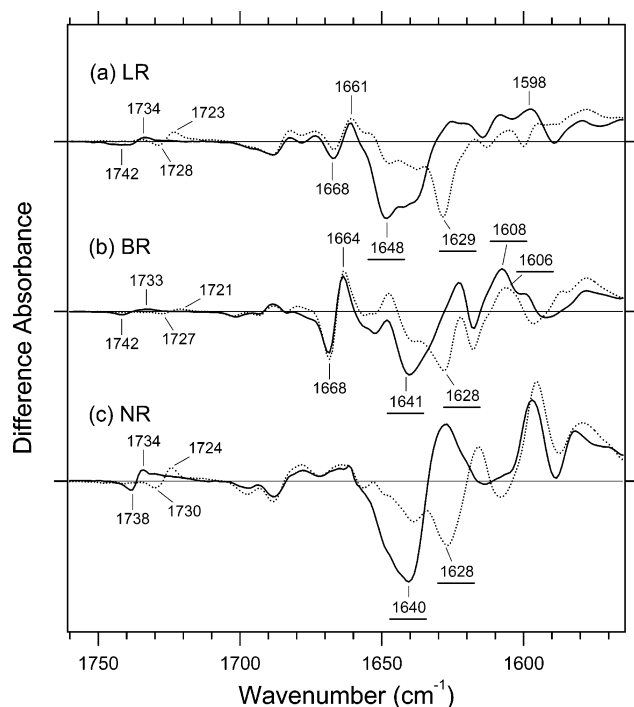


FIGURE 5: LR<sub>K</sub> minus LR (a), BR<sub>K</sub> minus BR (b), and NR<sub>K</sub> minus NR (c) spectra in the 1760–1565 cm<sup>-1</sup> region, being reproduced and expanded from Figure 2. Most of bands in this region can be ascribed to vibrations of the protein moiety. The underlined peaks are C=N stretching vibrations of the chromophore. The sample was hydrated with H<sub>2</sub>O (—) or D<sub>2</sub>O (···). One division of the y-axis corresponds to 0.004 absorbance unit.

that the retinal distortions upon LR<sub>K</sub> formation are localized in the Schiff base region, as in BR<sub>K</sub>.

Figure 5 shows the LR<sub>K</sub> minus LR (a), BR<sub>K</sub> minus BR (b), and NR<sub>K</sub> minus NR (c) spectra in the 1760–1565 cm<sup>-1</sup> region, where most of the bands originate from vibrations of the protein. One exception is the C=N stretching vibration of the retinal Schiff base that appears in the 1650–1600 cm<sup>-1</sup> region. In BR, the C=N stretch has been observed at 1641 cm<sup>-1</sup> in H<sub>2</sub>O and at 1628 cm<sup>-1</sup> in D<sub>2</sub>O (Figure 5b) (48). This frequency upshift in H<sub>2</sub>O is caused by coupling to the N–H bending vibration of the Schiff base, and the difference in frequency between H<sub>2</sub>O and D<sub>2</sub>O has been regarded as a measure of the hydrogen-bonding strength of the Schiff base (38, 49, 50). The small difference in BR<sub>K</sub> (1608 cm<sup>-1</sup> in H<sub>2</sub>O vs 1606 cm<sup>-1</sup> in D<sub>2</sub>O) has been interpreted in terms of the lack of a hydrogen bond for the Schiff base nitrogen after photoisomerization (40, 51). The corresponding bands of NR were observed at 1640 and 1628 cm<sup>-1</sup> in H<sub>2</sub>O and D<sub>2</sub>O, respectively (Figure 5c) (31). The D<sub>2</sub>O-sensitive negative band was also observed for LR, with frequencies of 1648 and 1629 cm<sup>-1</sup> in H<sub>2</sub>O and D<sub>2</sub>O, respectively (Figure 5a). These IR bands are close in frequency to the Raman bands of LR at 1648 and 1627 cm<sup>-1</sup> (22), which were earlier assigned to the C=N stretches of the Schiff base in H<sub>2</sub>O and D<sub>2</sub>O, respectively. The IR frequency shift in LR (19 cm<sup>-1</sup>) is larger than those in BR (13 cm<sup>-1</sup>) and NR (12 cm<sup>-1</sup>), suggesting that the hydrogen bond of the Schiff base is stronger in LR than in BR and NR. It should, however, be noted that the negative 1648 cm<sup>-1</sup> band has a shoulder at the lower-frequency side, which makes the estimate less accurate. We reexamined the hydrogen-bonding strength of the Schiff base by the analysis of the N–D stretch vibrations,

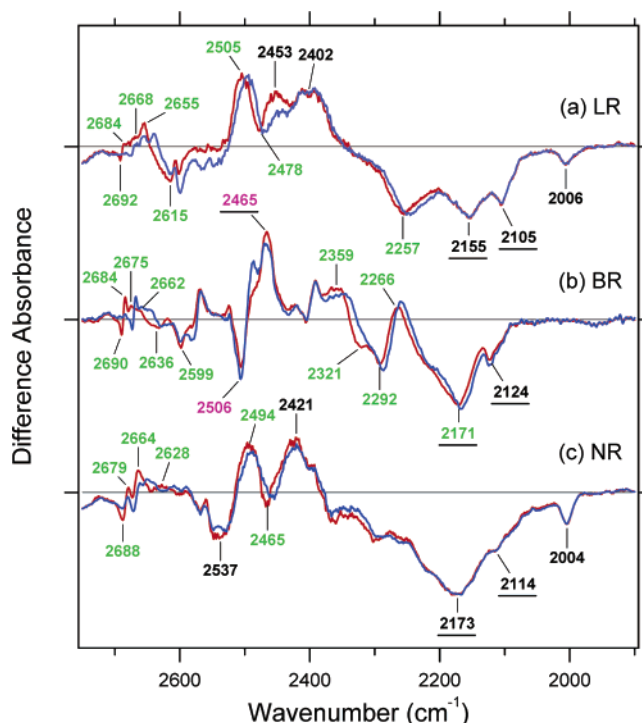


FIGURE 6: LR<sub>K</sub> minus LR (a), BR<sub>K</sub> minus BR (b), and NR<sub>K</sub> minus NR (c) spectra in the 2750–1900 cm<sup>-1</sup> region. The sample was hydrated with D<sub>2</sub>O (red lines) or D<sub>2</sub><sup>18</sup>O (blue lines). Spectra in panels b and c are reproduced from Furutani et al. (31). Green-labeled frequencies correspond to those identified as water stretching vibrations. In BR (b), purple-labeled frequencies are O–D stretches of Thr89 (59, 60) while the underlined frequencies are N–D stretches of the Schiff base (52). One division of the y-axis corresponds to 0.00065 absorbance unit.

believed to be a more direct monitor than the C=N stretch (52) (see below). Because it is also difficult to locate the C=N stretching mode in LR<sub>K</sub> (Figure 5a), the spectral analysis of the X–D stretching frequencies becomes even more relevant for providing clear information about the Schiff base environment.

**Comparison of the Vibrational Bands of the Protein Moiety among LR, BR, and NR.** The bands in Figure 5 (except for the C=N stretching vibrations of the Schiff base) come from the protein moieties of LR, BR, and NR. In BR, the 1742 (–)/1733 (+) cm<sup>-1</sup> bands in H<sub>2</sub>O are shifted to 1727 (–)/1721 (+) cm<sup>-1</sup> in D<sub>2</sub>O, which was previously assigned to the C=O stretches of Asp115 (53). Corresponding amino acids are Asp169 in LR and Asp161 in NR, and similar bands were observed at 1750–1720 cm<sup>-1</sup> (Figure 5a,c). This indicates that the aspartic acid at this position is protonated in both LR and NR, and the hydrogen-bonding alterations upon retinal isomerization are similar. It is, however, noted that the frequencies in LR are similar to those in BR, and those in NR are considerably different. This tendency is consistent with that for the chromophore bands.

The bands at 1668 (–)/1664 (+) cm<sup>-1</sup> in BR are highly dichroic (23) and appear in the typical frequency region of the amide I vibrations of the α<sub>II</sub> helix (Figure 5b) (54), which is probably located in the transmembrane region. Similar spectral changes at 1668 (–)/1661 (+) cm<sup>-1</sup> were also observed for LR (Figure 5a), whereas there are no such bands for NR (Figure 5c).

**Comparison of the Structure of the Schiff Base Region among LR, BR, and NR.** Figure 6 shows the LR<sub>K</sub> minus LR

(a),  $\text{BR}_K$  minus BR (b), and  $\text{NR}_K$  minus NR (c) spectra in the 2750–1900  $\text{cm}^{-1}$  region, which contains the X–D stretching vibrations of protein and water molecules. A spectral comparison between the samples hydrated with  $\text{D}_2\text{O}$  and  $\text{D}_2^{18}\text{O}$  reveals O–D stretching vibrations of water molecules which change in frequency upon retinal photoisomerization. The vibrational bands exhibiting isotope-induced downshifts can be assigned to the O–D stretching vibrations of water (labeled in green; Figure 6). In BR, six negative peaks at 2690, 2636, 2599, 2321, 2292, and 2171  $\text{cm}^{-1}$  were earlier assigned to vibrations of water molecules. The bands are widely distributed over the possible frequency range for stretching vibrations of water (Figure 6b). Since the frequencies of the negative peaks at 2321, 2292, and 2171  $\text{cm}^{-1}$  are much lower than those of fully hydrated tetrahedral water molecules (24, 55, 56), the hydrogen bonds of those water molecules must be very strong, possibly indicating their association with negative charges. Indeed, we assigned the 2171  $\text{cm}^{-1}$  band to the O–D group of a water molecule associated with deprotonated Asp85 (25). In addition, we recently concluded that six vibrational bands can be assigned to six O–D stretching vibrations of the three water molecules present in the Schiff base region (27).

Interestingly, water vibrations in archaeal rhodopsins from eukaryotes are remarkably different from those of BR. In NR, only two negative peaks that can be assigned to the O–D stretching vibrations of water at 2688 and 2465  $\text{cm}^{-1}$  were observed (31) (Figure 6c). The water stretching vibrations of  $\text{NR}_K$  were assigned to the bands at 2679, 2664, 2628, and 2494  $\text{cm}^{-1}$ . In the case of LR, three negative bands were observed at 2692, 2615, and 2257  $\text{cm}^{-1}$  (Figure 6a). In addition, the negative peak of water at 2478  $\text{cm}^{-1}$  is probably obscured by large positive bands. Corresponding positive bands are located at 2684, 2668, 2655, and 2505  $\text{cm}^{-1}$ . It should be emphasized that there are no water bands in the  $<2400$   $\text{cm}^{-1}$  region for NR (Figure 6c), whereas LR possesses the O–D stretch of water at 2257  $\text{cm}^{-1}$  (Figure 6a). Therefore, in contrast to NR, LR contains a strongly hydrogen-bonded water molecule. Previously, we examined the presence of strongly hydrogen-bonded water molecules in various rhodopsins of the haloarchaeal type. Strongly hydrogen-bonded water molecules were found in BR (24), various BR mutants except for D85N and D212N (25, 27), and *ppR* (28), which can pump protons in the transducer-free form. In contrast, they were not found in HR (29) and NR (31), which, together with the D85N and D212N mutants of BR, have no proton-pumping ability (57, 58). On the basis of these observations, we have proposed a working hypothesis that the existence of strongly hydrogen-bonded water molecules is required for proton-pumping activity in type I rhodopsins. Since LR pumps protons (22), this FTIR result supports this working hypothesis.

The frequency region shown in Figure 6 also contains X–D stretching vibrations other than those of water molecules. In the  $\text{BR}_K$  minus BR spectrum, the bands at 2506 (–)/2465 (+)  $\text{cm}^{-1}$  labeled in purple and the underlined bands at 2465 (+), 2171 (–), and 2124 (–)  $\text{cm}^{-1}$  were assigned to the O–D stretching vibrations of Thr89 (59, 60) and the N–D stretching vibrations of the retinal Schiff base (52), respectively (Figure 6b). Thus, the negative 2171  $\text{cm}^{-1}$  band contains both the O–D stretch of water and the N–D stretch of the Schiff base. The bands at 2292 (–)/2266 (+)  $\text{cm}^{-1}$  also contain the N–D stretching vibration of Arg82

(61). In the  $\text{LR}_K$  minus LR spectrum, there are five bands at 2453 (+), 2402 (+), 2155 (–), 2105 (–), and 2006 (–)  $\text{cm}^{-1}$ , which do not originate from water vibrations (Figure 6a). Though not assigned directly by use of the labeled protein, the bands at 2155 and 2105  $\text{cm}^{-1}$  are likely to originate from N–D stretching of the Schiff base. The frequencies are similar, but considerably lower than those in BR (2171 and 2124  $\text{cm}^{-1}$ ) and NR (2173 and 2114  $\text{cm}^{-1}$ ) (Figure 6b,c). Therefore, the hydrogen-bonding strength of the Schiff base in LR is slightly greater than those in BR and NR, which is consistent with the results obtained for the C=N stretching vibrations shown above (Figure 5). The spectral shape of the  $\text{LR}_K$  minus LR (Figure 6a) clearly shows that the N–D stretch of the Schiff base is located at the higher-frequency side in  $\text{LR}_K$ , indicating its weakened hydrogen bond. We consider either the 2453 or 2402  $\text{cm}^{-1}$  band to be the candidate for the N–D stretch in  $\text{LR}_K$ . In any case, the hydrogen-bonding alterations of the protonated Schiff base are essentially identical between LR and BR, where the hydrogen bond is disrupted upon retinal isomerization.

## DISCUSSION

In this paper, we studied the structural changes of LR following retinal photoisomerization by means of low-temperature Fourier transform infrared (FTIR) spectroscopy, and compared the obtained spectra with those for BR and NR. Among fungal rhodopsins, proton-pumping activity was found for only LR and not for NR (20, 22). It is instructive to see whether their functional differences can be explained in terms of their structures.

Figure 1 shows that the primary structure of LR is highly homologous to that of NR, but not to that of BR. It is reasonable that fungal rhodopsins, LR and NR, possess a high degree of homology, being distinct from archaeal BR. Tertiary structures of LR and NR have not been determined, but they must be quite similar to that of BR. According to the BR structure, there are 25 amino acids within 5 Å of the retinal chromophore as shown in Figure 1. There is only one amino acid which differs among the corresponding 25 amino acids of LR and NR (Ser141 of BR is Ala196 in LR and Gly189 in NR). In contrast, there are five amino acids that are different among the corresponding 25 amino acids of LR and BR (Figure 1). These results may suggest that the local structure around the retinal chromophore in LR is similar to that in NR, but not in BR. However, this FTIR study revealed that the structure of this region and its structural changes upon retinal photoisomerization in LR are similar to those in BR, and not those in NR. Photoisomerization in LR yields the chromophore distortions in the Schiff base region like those in BR as shown in the HOOP region (Figure 4). Peptide backbone alterations in LR are also similar to those of BR (Figure 5). These results suggest that the local structural perturbations in the K state are not necessarily determined by local structural elements. Rather, distant amino acids and/or whole protein structure is the determinant of the structure and its structural changes. In the case of BR, local and distant protein structural changes were found by isotope labeling and mutational analysis (62). A similar study for fungal rhodopsins will identify the location of the protein structural changes for LR and NR.

As shown above, the primary structure is highly homologous between LR and NR, whereas the local structure and



structural changes of the chromophore are similar between LR and BR. The latter is coincident with the function, namely, the proton-pumping activity. Vibrations of internal water molecules may give a hint about the answer to the question on the structural determinants of the proton-pumping activity. A significant difference was seen for water bands among LR, BR, and NR. LR exhibits an O–D stretch of water at  $2257\text{ cm}^{-1}$ , indicating the presence of a strongly hydrogen-bonded water molecule (Figure 6). Such strongly hydrogen-bonded water molecules (O–D stretch at  $<2400\text{ cm}^{-1}$ ) were observed for BR, but not for NR.

Then, the location of the water in LR is interesting. A previous mutation study of BR revealed that the lowest water band at  $2171\text{ cm}^{-1}$  originates from the bridged water molecule between the Schiff base and counterion (Asp85) (25, 27). Since the frequency at  $2257\text{ cm}^{-1}$  for LR is very low as an O–D stretch of water, it is likely to interact with a negative charge. Therefore, the water may bridge the Schiff base and counterion (Asp139) also in LR. A mutation study of LR will provide more detailed information about the location of water molecules in the future.

On the basis of our FTIR studies of BR mutants and other rhodopsins, we have found a correlation between strongly hydrogen-bonded water molecules and proton-pumping activity. Among various BR mutant proteins we have studied, only D85N and D212N lack strongly hydrogen-bonded water molecules. Other BR mutants possess their O–D stretches at  $<2400\text{ cm}^{-1}$ , which includes T46V, R82Q, R82Q/D212N, T89A, D96N, D115N, Y185F, and E204Q (27). Among these mutants, only D85N and D212N do not pump protons under the experimental conditions for FTIR. Therefore, strongly hydrogen-bonded water molecules are only found in the proteins exhibiting proton-pumping activities. The correlation between proton pumping activity and strongly hydrogen-bonded water molecules is true not only for BR mutants but also for various rhodopsins. We systematically examined whether other rhodopsins possess strongly hydrogen-bonded water molecules. We found that BR and *pharaonis* phoborhodopsin (24, 26, 28), both of which pump protons, possess such water molecules (O–D stretch at  $<2400\text{ cm}^{-1}$  in  $\text{D}_2\text{O}$ ). In contrast, strongly hydrogen-bonded water molecules were not observed for halorhodopsin (29), and bovine rhodopsin (30). It is known that none of them pumps protons. Such comprehensive studies of archaeal and visual rhodopsins have thus revealed that strongly hydrogen-bonded water molecules are found only in the proteins exhibiting proton-pumping activities. Taken together with our recent results for LR and NR, it suggests that the strong hydrogen bonds of water molecules and their transient weakening may be essential for the proton-pumping function of rhodopsins.

## ACKNOWLEDGMENT

We thank Alex Idnurm and Barbara J. Howlett for providing DNA for the *Leptosphaeria ops* gene, as well as Doreen E. Culham and Janet M. Wood for assistance in subcloning *ops* gene. We thank Mikihiro Shibata for valuable discussions about the internal water molecules of BR.

## REFERENCES

- Spudich, J. L., Yang, C., Jung, K., and Spudich, E. N. (2000) Retinylidene proteins: Structures and functions from archaea to humans, *Annu. Rev. Cell Dev. Biol.* 16, 365–392.
- Idnurm, A., and Howlett, B. J. (2001) Characterization of an opsin gene from the ascomycete *Leptosphaeria maculans*, *Genome* 44, 167–171.
- Jung, K. H., and Spudich, J. L. (2004) Microbial rhodopsins: Transport and sensory proteins throughout the three domains of life, in *CRC Handbook of Organic Photochemistry and Photobiology* (Horspool, W. M., and Lenci, F., Eds.) Section II Photobiology, 2nd ed., pp 124/1–124/11, CRC Press, Boca Raton, FL.
- Nagel, G., Ollig, D., Fuhrmann, M., Kateriya, S., Musti, A. M., Bamberg, E., and Hegemann, P. (2002) Channelrhodopsin-1: A light-gated proton channel in green algae, *Science* 296, 2395–2398.
- Sineshchekov, O. A., Jung, K.-H., and Spudich, J. L. (2002) Two rhodopsins mediate phototaxis to low- and high-intensity light in *Chlamydomonas reinhardtii*, *Proc. Natl. Acad. Sci. U.S.A.* 99, 8689–8694.
- Ng, W. V., Kennedy, S. P., Mahairas, G. G., Berquist, B., Pan, M., Shukla, H. D., Lasky, S. R., Baliga, N. S., Thorsson, V., Sbrogna, J., Swartzell, S., Weir, D., Hall, J., Dahl, T. A., Welti, R., Goo, Y. A., Leithauser, B., Keller, K., Cruz, R., Danson, M. J., Hough, D. W., and Maddocks, D. (2000) Genome sequence of *Halobacterium* species NRC-1, *Proc. Natl. Acad. Sci. U.S.A.* 97, 12176–12181.
- Lanyi, J. K. (1997) Mechanism of ion transport across membranes, *J. Biol. Chem.* 272, 31209–31212.
- Haupts, U., Tittor, J., and Oesterhelt, D. (1999) Closing in on bacteriorhodopsin: Progress in understanding the molecule, *Annu. Rev. Biophys. Biomol. Struct.* 28, 367–399.
- Lanyi, J. K. (1990) Halorhodopsin, a light-driven electrogenic chloride-transport system, *Physiol. Rev.* 70, 319–330.
- Hoff, W. D., Jung, K. H., and Spudich, J. L. (1997) Molecular mechanism of photosignaling by archaeal sensory rhodopsins, *Annu. Rev. Biophys. Biomol. Struct.* 26, 223–258.
- Kamo, N., Shimono, K., Iwamoto, M., and Sudo, Y. (2001) Photochemistry and photoinduced proton-transfer by *pharaonis* phoborhodopsin, *Biochemistry (Moscow)* 66, 1277–1282.
- Sasaki, J., and Spudich, J. L. (2000) Proton transport by sensory rhodopsins and its modulation by transducer-binding, *Biochim. Biophys. Acta* 1460, 230–239.
- Brown, L. S. (2004) Fungal rhodopsins and opsin-related proteins: Eukaryotic homologues of bacteriorhodopsin with unknown functions, *Photochem. Photobiol. Sci.* 3, 555–565.
- Beja, O., Aravind, L., Koonin, E. V., Suzuki, M. T., Hadd, A., Nguyen, L. P., Jovanovich, S. B., Gates, C. M., Feldman, R. A., Spudich, J. L., Spudich, E. N., and DeLong, E. F. (2000) Bacterial rhodopsin: Evidence for a new type of phototrophy in the Sea, *Science* 289, 1902–1906.
- de la Torre, J. R., Christianson, L. M., Béjà, O., Suzuki, M. T., Karl, D. M., Heidelberg, J., and DeLong, E. F. (2003) Proteorhodopsin genes are distributed among divergent marine bacterial taxa, *Proc. Natl. Acad. Sci. U.S.A.* 100, 12830–12835.
- Jung, K. H., Trivedi, V. D., and Spudich, J. L. (2003) Demonstration of a sensory rhodopsin in eubacteria, *Mol. Microbiol.* 47, 1513–1522.
- Bieszke, J. A., Braun, E. L., Bean, L. E., Kang, S., Natvig, D. O., and Borkovich, K. A. (1999) The *nop-1* gene of *Neurospora crassa* encodes a seven transmembrane helix retinal-binding protein homologous to archaeal rhodopsins, *Proc. Natl. Acad. Sci. U.S.A.* 96, 8034–8039.
- Okamoto, O. K., and Hastings, J. W. (2003) Novel dinoflagellate clock-related genes identified through microarray analysis, *J. Phycol.* 39, 519–526.
- Bieszke, J. A., Spudich, E. N., Scott, K. L., Borkovich, K. A., and Spudich, J. L. (1999) A eukaryotic protein, NOP-1, binds retinal to form an archaeal rhodopsin-like photochemically reactive pigment, *Biochemistry* 38, 14138–14145.
- Brown, L. S., Dioumaev, A. K., Lanyi, J. K., Spudich, E. N., and Spudich, J. L. (2001) Photochemical reaction cycle and proton transfers in *Neurospora* rhodopsin, *J. Biol. Chem.* 276, 32495–32505.
- Bergo, V., Spudich, E. N., Spudich, J. L., and Rothschild, K. J. (2002) A Fourier transform infrared study of *Neurospora* rhodopsin: Similarities with archaeal rhodopsins, *Photochem. Photobiol.* 76, 341–349.
- Waschuck, S. A., Bezerra, A. G., Jr., Shi, L., and Brown, L. S. (2005) *Leptosphaeria* rhodopsin: Bacteriorhodopsin-like proton pump from a eukaryote, *Proc. Natl. Acad. Sci. U.S.A.* 102, 6879–6883.

23. Kandori, H., Kinoshita, N., Shichida, Y., and Maeda, A. (1998) Protein structural changes in bacteriorhodopsin upon photoisomerization as revealed by polarized FTIR spectroscopy, *J. Phys. Chem. B* 102, 7899–7905.
24. Kandori, H., and Shichida, Y. (2000) Direct observation of the bridged water stretching vibrations inside a protein, *J. Am. Chem. Soc.* 122, 11745–11746.
25. Shibata, M., Tanimoto, T., and Kandori, H. (2003) Water molecules in the Schiff base region of bacteriorhodopsin, *J. Am. Chem. Soc.* 125, 13312–13313.
26. Tanimoto, T., Furutani, Y., and Kandori, H. (2003) Structural changes of water in the Schiff base region of bacteriorhodopsin: Proposal of a hydration switch model, *Biochemistry* 42, 2300–2306.
27. Shibata, M., and Kandori, H. (2005) FTIR studies of internal water molecules in the Schiff base region of bacteriorhodopsin, *Biochemistry* 44, 7406–7413.
28. Kandori, H., Furutani, Y., Shimono, K., Shichida, Y., and Kamo, N. (2001) Internal water molecules of *pharaonis* phoborhodopsin studied by low-temperature infrared spectroscopy, *Biochemistry* 40, 15693–15698.
29. Shibata, M., Muneda, N., Ihara, K., Sasaki, T., Demura, M., and Kandori, H. (2004) Internal water molecules of light-driven chloride pump proteins, *Chem. Phys. Lett.* 392, 330–333.
30. Furutani, Y., Shichida, Y., and Kandori, H. (2003) Structural changes of water molecules during the photoactivation processes in bovine rhodopsin, *Biochemistry* 42, 9619–9625.
31. Furutani, Y., Bezerra, A. G., Jr., Waschuk, S., Sumii, M., Brown, L. S., and Kandori, H. (2004) FTIR spectroscopy of the K photointermediate of *Neurospora* rhodopsin: Structural changes of the retinal, protein, and water molecules after photoisomerization, *Biochemistry* 43, 9636–9646.
32. Shimono, K., Ikeura, Y., Sudo, Y., Iwamoto, M., and Kamo, N. (2001) Environment around the chromophore in *pharaonis* phoborhodopsin: Mutation analysis of the retinal binding site, *Biochim. Biophys. Acta* 1515, 92–100.
33. Kandori, H., Shimono, K., Sudo, Y., Iwamoto, M., Shichida, Y., and Kamo, N. (2001) Structural changes of *pharaonis* phoborhodopsin upon photoisomerization of the retinal chromophore: Infrared spectral comparison with bacteriorhodopsin, *Biochemistry* 40, 9238–9246.
34. Maeda, A., Iwasa, T., and Yoshizawa, T. (1977) Isomeric composition of retinal chromophore in dark-adapted bacteriorhodopsin, *J. Biochem.* 82, 1599–1604.
35. Kamo, N., Hazemoto, N., Kobatake, Y., and Mukohata, Y. (1985) Light and dark adaptation of halorhodopsin, *Arch. Biochem. Biophys.* 238, 90–96.
36. Tsuda, M., Nelson, B., Chang, C.-H., Govindjee, R., and Ebrey, T. G. (1985) Characterization of the chromophore of the third rhodopsin-like pigment of *Halobacterium halobium* and its photoproduct, *Biophys. J.* 47, 721–724.
37. Imamoto, Y., Shichida, Y., Hirayama, J., Tomioka, H., Kamo, N., and Yoshizawa, T. (1992) Chromophore configuration of *pharaonis* phoborhodopsin and its isomerization on photon absorption, *Biochemistry* 31, 2523–2528.
38. Aton, B., Doukas, A. G., Callender, R. H., Becher, B., and Ebrey, T. G. (1977) Resonance Raman studies of the purple membrane, *Biochemistry* 16, 2995–2999.
39. Maeda, A. (1995) Application of FTIR spectroscopy to the structural study on the function of bacteriorhodopsin, *Isr. J. Chem.* 35, 387–400.
40. Smith, S. O., Lugtenburg, J., and Mathies, R. A. (1985) Determination of retinal chromophore structure in bacteriorhodopsin with resonance Raman spectroscopy, *J. Membr. Biol.* 85, 95–109.
41. Maeda, A., Sasaki, J., Pfefferlér, J.-M., Shichida, Y., and Yoshizawa, T. (1991) Fourier transform infrared spectral studies on the Schiff base mode of all-*trans* bacteriorhodopsin and its photointermediates, K and L, *Photochem. Photobiol.* 54, 911–921.
42. Smith, S. O., Braiman, M. S., Myers, A. B., Pardo, J. A., Courtin, J. M. L., Winkler, C., Lugtenburg, J., and Mathies, R. A. (1987) Vibrational analysis of the all-*trans*-retinal chromophore in light-adapted bacteriorhodopsin, *J. Am. Chem. Soc.* 109, 3108–3125.
43. Gerwert, K., and Siebert, F. (1986) Evidence for light-induced 13-*cis*, 14-*s-cis* isomerization in bacteriorhodopsin obtained by FTIR difference spectroscopy using isotopically labeled retinals, *EMBO J.* 5, 805–811.
44. Mathies, R. A., Lin, S. W., Ames, J. B., and Pollard, W. T. (1991) From femtoseconds to biology: Mechanism of bacteriorhodopsin's light-driven proton pump, *Annu. Rev. Biophys. Biophys. Chem.* 20, 491–518.
45. Rothschild, K. J. (1992) FTIR difference spectroscopy of bacteriorhodopsin: Toward a molecular model, *J. Bioenerg. Biomembr.* 24, 147–167.
46. Siebert, F. (1995) Infrared spectroscopy applied to biochemical and biological problems, *Methods Enzymol.* 246, 501–526.
47. Gerwert, K. (1999) Molecular reaction mechanisms of proteins monitored by time-resolved FTIR-spectroscopy, *Biol. Chem.* 380, 931–935.
48. Siebert, F., and Mäntele, W. (1983) Investigation of the primary photochemistry of bacteriorhodopsin by low-temperature Fourier-transform infrared spectroscopy, *Eur. J. Biochem.* 130, 565–573.
49. Rodman-Gilson, H. S., Honig, B., Croteau, A., Zarrilli, G., and Nakanishi, K. (1988) Analysis of the factors that influence the C=N stretching frequency of polyene Schiff bases. Implications for bacteriorhodopsin and rhodopsin, *Biophys. J.* 53, 261–269.
50. Baasov, T., Friedman, N., and Sheves, M. (1987) Factors affecting the C=N stretching in protonated retinal Schiff base: A model study for bacteriorhodopsin and visual pigments, *Biochemistry* 26, 3210–3217.
51. Rothschild, K. J., Roepe, P., Lugtenburg, J., and Pardo, J. A. (1984) Fourier transform infrared evidence for Schiff base alteration in the first step of the bacteriorhodopsin photocycle, *Biochemistry* 23, 6103–6109.
52. Kandori, H., Belenky, M., and Herzfeld, J. (2002) Vibrational frequency and dipolar orientation of the protonated Schiff base in bacteriorhodopsin before and after photoisomerization, *Biochemistry* 41, 6026–6031.
53. Braiman, M. S., Mogi, T., Marti, T., Stern, L. J., Khorana, H. G., and Rothschild, K. J. (1988) Vibrational spectroscopy of bacteriorhodopsin mutants: Light-driven proton transport involves protonation changes of aspartic acid residues 85, 96, and 212, *Biochemistry* 27, 8516–8520.
54. Krimm, S., and Dwivedi, A. M. (1982) Infrared spectrum of the purple membrane: Clue to a proton conduction mechanism? *Science* 216, 407–408.
55. Monosmith, W. B., and Walrafen, G. E. (1984) Temperature dependence of the Raman hydroxyl-stretching overtone from liquid water, *J. Chem. Phys.* 81, 669–674.
56. Walrafen, G. E., and Fisher, M. R. (1986) Low-frequency Raman scattering from water and aqueous solutions: A direct measure of hydrogen-bonding, *Methods Enzymol.* 127, 91–105.
57. Mogi, T., Stern, L. J., Marti, T., Chao, B. H., and Khorana, H. G. (1988) Aspartic acid substitutions affect proton translocation by bacteriorhodopsin, *Proc. Natl. Acad. Sci. U.S.A.* 85, 4148–4152.
58. Moltke, S., Krebs, M. P., Mollaaghababa, R., Khorana, H. G., and Heyn, M. P. (1995) Intramolecular charge transfer in the bacteriorhodopsin mutants Asp85→Asn and Asp212→Asn: Effects of pH and anions, *Biophys. J.* 69, 2074–2083.
59. Kandori, H., Kinoshita, N., Yamazaki, Y., Maeda, A., Shichida, Y., Needleman, R., Lanyi, J. K., Bizounok, M., Herzfeld, J., Raap, J., and Lugtenburg, J. (1999) Structural change of threonine 89 upon photoisomerization in bacteriorhodopsin as revealed by polarized FTIR spectroscopy, *Biochemistry* 38, 9676–9683.
60. Kandori, H., Yamazaki, Y., Shichida, Y., Raap, J., Lugtenburg, J., Belenky, M., and Herzfeld, J. (2001) Tight Asp-85-Thr-89 association during the pump switch of bacteriorhodopsin, *Proc. Natl. Acad. Sci. U.S.A.* 98, 1571–1576.
61. Tanimoto, T., Shibata, M., Belenky, M., Herzfeld, J., and Kandori, H. (2004) Altered hydrogen bonding of Arg82 during the proton pump cycle of bacteriorhodopsin: A low-temperature polarized FTIR spectroscopic study, *Biochemistry* 43, 9439–9447.
62. Kandori, H., Kinoshita, N., Yamazaki, Y., Maeda, A., Shichida, Y., Needleman, R., Lanyi, J. K., Bizounok, M., Herzfeld, J., Raap, J., and Lugtenburg, J. (2000) Local and distant protein structural changes on photoisomerization of the retinal in bacteriorhodopsin, *Proc. Natl. Acad. Sci. U.S.A.* 97, 4643–4648.
63. Luecke, H., Schobert, B., Richter, H.-T., Cartailler, J. P., and Lanyi, J. K. (1999) Structure of bacteriorhodopsin at 1.55 Å resolution, *J. Mol. Biol.* 291, 899–911.
64. Thompson, J. D., Higgins, D. G., and Gibson, T. J. (1994) CLUSTAL W: Improving the sensitivity of progressive multiple sequence alignment through sequence weighting, position-specific gap penalties and weight matrix choice, *Nucleic Acids Res.* 22, 4673–4680.